PROCEEDINGS of the
23rd International Congress on Acoustics
9 to 13 September 2019 in Aachen, Germany

Comparison of sound pressure levels and reverberation times computed by the Boundary Element Method and the Radiosity Method

Christian STEUCK[(1)], Uwe M. STEPHENSON[(2)]

[(1)]HafenCity Universität Hamburg, Germany, christian.steuck@hcu-hamburg.de
[(2)]HafenCity Universität Hamburg, Germany, uwe.stephenson@hcu-hamburg.de

1st June 2019

Abstract

Boundary Element Method (BEM) and Radiosity Method (RadM) are established methods for numerical sound field computation. The BEM yields sound pressure amplitudes mainly for low frequencies, whereas for high frequencies geometrical methods are more efficient: ray and beam tracing and, well known in illumination simulation, the RadM. The latter, in contrast to the BEM, is based on an energy balance described by Kuttruff's integral equation. A comparison of BEM and RadM is interesting as both are based on a very similar data structure: a subdivision of the room's surface into a large number of patches and a matrix of factors describing the geometrical relationships between them. While the BEM requires surface impedances, the RadM uses absorption degrees assuming perfectly diffusely reflecting walls and yields, in its stationary version, the illumination distribution and from that the local sound energy densities and levels. Its iterative solution in time domain yields energy decay curves and thus reverberation times. With the BEM, these are computed by inverse Fourier Transform. A set of rooms with different local distributions of the absorption coefficient is examined, the results of both methods are compared with regard to sound pressure level and reverberation time.

Keywords: numerical acoustics, room acoustics, boundary elements, radiosity, reverberation time, sound pressure levels, integral equation, patches

1 INTRODUCTION

Boundary Element Method (BEM) and the Radiosity Method (RadM) are established methods of numerical acoustics, the latter also in room acoustics though extremely different and in a different application. The BEM [1,2] is a low frequency method for rooms of a few wavelengths extension as in many sound radiation problems of machine noise and car cabin acoustics; it requires surface impedances as boundary conditions, the considered quantity is the sound pressure p on the room surface and its coherent superposition in the frequency domain. The RadM like mirror image source method [3], ray and beam tracing [4,7] is valid only for rooms of large dimensions compared with the wavelength such that incoherent, i.e. energetic superposition is assumed. The considered quatitiy is the irradiation strength B on the room surface. It is often used as an extension to ray tracing to compute reverberation times [5,6]. Usually octave band averaged absorption degrees are given, the objective quantity is the irradiation strength B on the room surface.

Both methods have in common that an integral equation over the surface S of a volume (room) V is solved by discretization: Kirchhoff's in BEM, Kuttruff's in RadM. For that purpose the room surface is subdivided into a large number of small "patches" of approximately same size, typically triangles or squares and to consider their mutual interaction in a matrix whose elements contain Green's function (BEM) or "transition factors" (RadM), both depend mainly on geometry.

While for the BEM the patches should be smaller than a sixth of the wavelength, the RadM patches are usually much larger; they should be smaller than a tenth of the mean free path length $\Lambda = 4V/S$. Furthermore, the pairwise consideration in RadM inherently means perfectly diffuse, i.e. "forgetting" reflections independent from the incident direction of sound. RadM is only valid above the Schroeder-frequency, BEM can be applied

for frequencies up to a value that is limited by the computational effort only.

With this paper, a first attempt is made, to compare these very different and yet similar methods. As a typical example of application, computed sound fields, sound pressure levels and reverberation times in some small reverberation chambers are compared, without and with absorber. Very different results are expected and discussed.

2 THEORY

Both methods have in common that there are four types of irradiation to be considered:

1) from a source point within the volume V to the surface S; 2) wall-wall (patch-patch) interaction; 3) wall-receiver (point in V); 4) direct source-receiver. 1) and 2) are summarized in one equation resp. one computational step, the same with 3) and 4).

To solve the resulting integral equations, first the surface is discretized into small patches, and an interaction matrix between all patches is pre-computed. Then, first, with the BEM the sound pressure $\underline{p}(\vec{r},f)$ over the surface resp. p_{li} is computed by solving a linear equation system, or, iteratively, in the RadM the irradiation strength $B(\vec{r},t)$ resp. B_{li} is computed. Then, from that, $\underline{p}(\vec{r}_r,f)$ the final result (after Fourier transform pressure $p(\vec{r}_r,t)$) resp. intensity $I(\vec{r}_r,t)$ at the receivers. (For variables see below.)

2.1 Variables in both methods

S = room surface, V = room volume; quantities with ': source side

points on S: $\vec{r}'$ = source, $\vec{r}$ = receiver patch, points in V: $\vec{r}_s$ = source, $\vec{r}_r$ = receiver, (see fig. 1a); polar angles related to surface normal at points $\vec{r}$ and $\vec{r}'$ (see fig. 1b): θ and θ', respectively.

variable distances: $R = |\vec{r}' - \vec{r}|$, $R_s = |\vec{r}_s - \vec{r}|$, $R_r = |\vec{r}_r - \vec{r}|$.

differential surfaces: $\mathrm{d}S'(\vec{r}')$, $\mathrm{d}S(\vec{r})$.

After discretization of the surface into N patches of approximately same area: index i source patch, k receiver patch. surfaces ΔS_i resp. ΔS_k on source resp. receiver side; with double indices: first for source, second for receiver;

discretized distances from/to the centroids of ΔS_i, resp. ΔS_k: R_{ik}, R_{sk}, R_{ir}, R_{sr}, patch centroids $\vec{c}_i$, $\vec{c}_k$.

polar angles measured at the centroids of ΔS_i resp. ΔS_k into the direction of the other: θ_{ik}, θ_{ki}.

physical quantities: given constants: sound power at source: $P(t)$, BEM: complex impedance $\underline{Z}(\vec{r}')$ resp. discrete Z_i, RadM: energetical reflection degree $\rho(\vec{r}')$ resp. ρ_i. Underlining indicates complex quantities.

to be computed: BEM: sound pressure $\underline{p}(r,f)$ resp. discrete $\underline{p}_{l,i}$, RadM: irradiation strength $B(\vec{r},t)$ resp. discrete B_{li}. l = number of time interval; $\underline{p}$, B = column vectors.

finally to be computed: sound pressure $p(\vec{r}_r,t)$ resp. intensity at receiver $I(\vec{r},t)$ resp. discrete I_{li}.

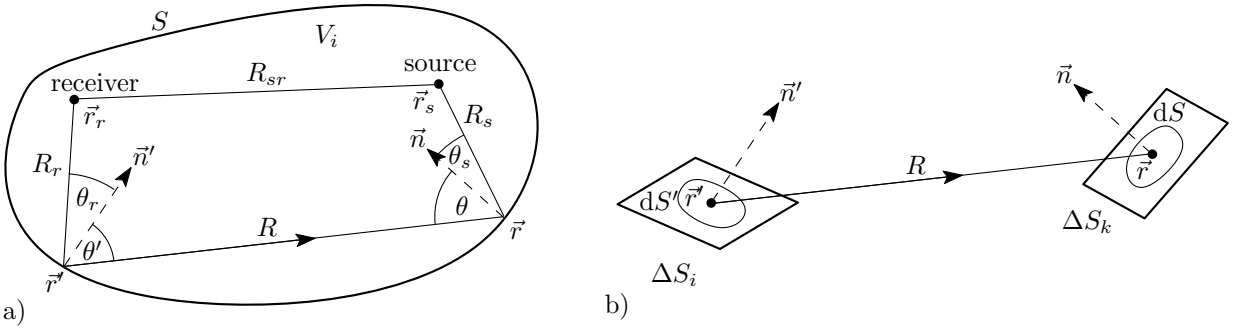

Figure 1. Geometrical setup relevant for both, BEM and RadM. a) overview, b) detail

2.2 Boundary Element Method (BEM)

Wave propagation is described by the Helmholtz equation

$$\nabla^2 \underline{p}(\vec{r},f) + k_w^2 \underline{p}(\vec{r},f) = 0. \tag{1}$$

Here the time convention is $\exp(j\omega t)$. Equation (1) has to be solved for the given boundary conditions for all frequencies resp. wave-numbers $k_w = \omega/c$, where $\omega = 2\pi f$ is the angular frequency, and c is the sound speed in air (340m/s). The fundamental solution, given a point source in $\vec{r}'$ results from applying (1) to Greens's function

$$\underline{g}(\vec{r},\vec{r}') = \frac{e^{-jk_w R}}{4\pi R}. \tag{2}$$

The pressure $\underline{p}$ can be formally split up into a scattered part and an incident part [1]:

$$\underline{p} = \underline{p}_{scat} + \underline{p}_{inc}. \tag{3}$$

Here "scattered" means reflected in any direction, not to be confused with scattering in contrast to geometrical reflection in geometrical acoustics. $\underline{p}_{inc}$ introduces the sound source (as with the RadM a sound power P is introduced), it is the source's free sound field. Here a point source was used ($1/r^2$-law). With the help of Green's second identity [1] applied each for $\underline{p}_{inc}$ and $\underline{p}_{scat}$ transforming a volume into a surface integral and inserting (1) yields Kirchhoff's integral equation

$$\int_S \left(\underline{p}(\vec{r}')\vec{n}'(\vec{r}') \cdot \nabla \underline{g}(\vec{r},\vec{r}') + j\omega\rho_a \underline{g}(\vec{r},\vec{r}') \underline{p}(\vec{r}')/\underline{Z}(\vec{r}') \right) \, \mathrm{d}S(\vec{r}') = \begin{cases} -\frac{1}{2}\underline{p}(\vec{r}) + \underline{p}_{inc}(\vec{r}), & \text{if } \vec{r} \text{ on } S, \\ -\underline{p}(\vec{r}) + \underline{p}_{inc}(\vec{r}), & \text{if } \vec{r} \text{ in } V_i. \end{cases} \tag{4}$$

Note that in (4) $\nabla \underline{p}$ has been substituted by $-j\omega\rho_a \underline{p}(\vec{r}')/\underline{Z}(\vec{r}')$ where ρ_a is the density of air (1.2 kg/m^3) and $\underline{Z}(\vec{r}')$ is the wall impedance.

After discretization, these integral equations (4) are solved in two main steps, as mentioned in 2.1 and described in 3.1.

Repeating this for several frequencies yields the room's transfer function and, after inverse Fourier transform and frequency band filtering, its impulse response.

2.3 Radiosity Method RadM

Kuttruff's integral equation (7) describes the mutual irradiation of infinitesimal surface elements; its solution is the radiation strength $B(\vec{r},t)$ on the surface ($\vec{r} \in S$) where B is defined as incident perpendicular to a surface and therefore relates to the intensity I via $B = I\cos\theta$. Each surface element $\mathrm{d}S(\vec{r})$ receives sound energy from all other elements $\mathrm{d}S'(\vec{r}')$ at distances R delayed by the times R/c. The total ammount of sound power sent from $\mathrm{d}S'$ is $\mathrm{d}P = \rho(\vec{r}')B(\vec{r}',t-R/c)\mathrm{d}S'(\vec{r}')$ with a local degree of reflection of $\rho(\vec{r}')$. According to Lambert's law the sound power emitted per solid angle $\mathrm{d}\Omega$ is

$$\mathrm{d}P'(\vec{r},t-R/c) = \rho(\vec{r}')\frac{\cos\theta'}{\pi} B(\vec{r}',t-R/c)\mathrm{d}S'(\vec{r}') \tag{5}$$

causing at a distance R an intensity of $I(\vec{r},t) = \mathrm{d}P'/R^2$ and thus an irradiation strength of

$$\mathrm{d}B(\vec{r},t) = \rho(\vec{r}')\frac{\cos\theta\cos\theta'}{\pi} B(\vec{r}',t-R/c)\mathrm{d}S'(\vec{r}'). \tag{6}$$

The sum of all contributions from the $\mathrm{d}S'(\vec{r}')$ including the direct sound from an omnidirectional source with power $P(t)$ yileds Kuttruff's integral equation

$$B(\vec{r},t) = \int_S \frac{\cos\theta\cos\theta'}{\pi R^2}\rho(\vec{r}')B(\vec{r}') \, \mathrm{d}S'(\vec{r}') + \frac{P(t-R_s/c)\cos\theta_s}{4\pi R_s^2}. \tag{7}$$

In an analogous way the incident intensity at the receiver point $I(\vec{r}_r)$ is obtained by summing the contributions of all wall elements and of the sound source:

$$I(\vec{r}_r,t) = \int_S \frac{\cos\theta_s'}{\pi R_r^2}\rho(\vec{r}')B(\vec{r}',t-R_s/c)\ \mathrm{d}S'(\vec{r}') + \frac{P(t-R_{sr}/c)}{4\pi R_{sr}^2}. \tag{8}$$

3 NUMERICAL IMPLEMENTATION

3.1 Boundary element method

In the patch based formulation of BEM each patch is assigned the valuees $\underline{p}_k$ and $\underline{Z}_k$ of pressure and impedance, respectively, hence the discretization of (4) is

$$-\frac{1}{2}\underline{p}_i + \underline{p}_{inc,i} = \sum_{k=1}^{N}\left(\int_{\Delta S_k}\vec{n}'(\vec{r}')\cdot\nabla\underline{g}(\vec{r},\vec{r}')\ \mathrm{d}S(\vec{r}')\right)\underline{p}_k + \left(j\omega\rho_a/\underline{Z}_k\int_{\Delta S_k}\underline{g}(\vec{r},\vec{r}')\ \mathrm{d}S(\vec{r}')\right)\underline{p}_k,\quad i=1,\ldots,N. \tag{9}$$

Empirically, $\underline{g}$ and $\nabla\underline{g}$ can be assumed to be constant on each patch if the length of the patches does not excede 1/6 of the wave length. Therefore the integrand in (9) is evaluated at the centroids $\vec{c}_i$ and $\vec{c}_k$ $(i,k=1,\ldots,N)$ of the patches (except for $i=k$). Thus (9) simplifies to:

$$-\frac{1}{2}\underline{p}_i + \underline{p}_{inc,i} = \sum_{k=1}^{N}\left(\vec{n}_k'\cdot\nabla\underline{g}(\vec{c}_i,\vec{c}_k) + j\omega\rho_a/Z_i\underline{g}(\vec{c}_i,\vec{c}_k)\right)\ \Delta S_k p_k. \tag{10}$$

In the case $i=k$ both, $\underline{g}$ and $\nabla\underline{g}$ become singular, yet the singularities can be fixed [1,2]. Finally the system of equation reads: $\underline{A}\vec{\underline{p}} = \vec{\underline{p}}_{inc}$, where

$$\underline{A}_{ik} = \begin{cases}\left(\vec{n}_k'\cdot\nabla\underline{g}(\vec{c}_i,\vec{c}_k) + j\omega\rho_a/Z_k\underline{g}(\vec{c}_i,\vec{c}_k)\right)\ \Delta S_k, & \text{if } i\neq k,\\ \frac{1}{2} - \frac{\rho_a c}{2}(\exp(-jk_w\sqrt{\Delta S_k/\pi})-1), & \text{if } i=k,\end{cases} \tag{11}$$

and $\vec{\underline{p}}$ is the column vector of the pressure values $\underline{p}_k$ at the patch centroids and the $\underline{p}_{inc,i}$ summarizes the pressure at the patch centroids due the source. Once the system is solved the pressure at the receiver positions at the frequency ω is obtained by executing the integration in (4) numerically for the case $\vec{r}=\vec{r}_r\in V_i$, i.e. replacing $\vec{c}_i$ by $\vec{r}_r$:

$$\underline{p}(\vec{r}_r,f) = -\sum_{k=1}^{N}\left(\vec{n}_k'\cdot\nabla\underline{g}(\vec{c}_k,\vec{r}_r) + j\omega\rho_a/\underline{Z}_k\underline{g}(\vec{c}_k,\vec{r}_r)\right)\ \Delta S_k + \underline{p}_{inc}(\vec{r}_r). \tag{12}$$

The sound pressure values at the receiver points, $\underline{p}(\vec{r}_r,f)$, are computed for all frequencies of the desired frequency band. To get impulse responses (FIR) $p(\vec{r}_r,t)$, discretized p_l, the $\underline{p}(\vec{r}_r,f)$ have to be Fourier transformed and band pass filtered.

3.2 Radiosity Method

The discretized version of Kuttruff's integral equation (7) assuming irradiation strengths and absorption coefficients to be constant on each patch reads

$$B_k(t) = \sum_{i=1,i\neq k}^{N}\left(\int_{\Delta S_i}\frac{\cos\theta\cos\theta'}{\pi R^2}\ \mathrm{d}S'(\vec{r}')\right)\rho_i B_i(t-R/c) + \frac{P(t-R_{s,k}/c)\cos\theta_{s,k}}{4\pi R_{s,k}^2}, \tag{13}$$

Assigning the right hand side of (13) to $B_k(t)$ implicitely means to assume that $\cos\theta = \text{const}$ for all $\vec{r} \in \Delta S_k$ although ΔS_k is a finite area. Therefore a further integration over the receiving patch ΔS_k is needed, interpretable as an averaging on ΔS_k:

$$B_k(t) = \frac{1}{\Delta S_k} \int\limits_{\Delta S_k} \sum_{i=1, i\neq k}^{N} \int\limits_{\Delta S_i} \frac{\cos\theta \cos\theta'}{\pi R^2} \, \mathrm{d}S'(\vec{r}') \, \mathrm{d}S(\vec{r}) \rho_i B_i(t - R/c) + \frac{P(t - R_{s,k}/c)\cos\theta_{s,k}}{4\pi R_{s,k}^2}. \tag{14}$$

Changing the order of summation and integration eq. (14) can be written as

$$B_k(t) = \sum_{i=1}^{N} \rho_i g_{ik} B_i(t - R/c) + \frac{P(t - R_{s,k}/c)\cos\theta_{s,k}}{4\pi R_{s,k}^2}, \tag{15}$$

where

$$g_{ik} = \frac{1}{\Delta S_k} \int\limits_{\Delta S_k} \int\limits_{\Delta S_i} \frac{\cos\theta \cos\theta'}{\pi R^2} \, \mathrm{d}S'(\vec{r}') \, \mathrm{d}S(\vec{r}), \text{ if } i \neq k; \quad g_{ii} = 0. \tag{16}$$

The transition factors g_{ik} can be interpreted as the fraction of sound power propagated from patch i *to patch* k in the total sound power propagated from patch i *to all patches*.

Transition factors g_{ik}: From the definition of a solid angle it follows that

$$\Omega_{ik}(\vec{r}) = \int\limits_{\Delta S_i} \frac{\cos\theta'}{R^2} \, \mathrm{d}S'(\vec{r}') \tag{17}$$

is the solid angle that ΔS_i covers as seen from a point $\vec{r}$ in ΔS_k. Hence

$$g_{ik} = \frac{\cos\theta_{ik}}{\pi} \Omega_{ik}. \tag{18}$$

It can be calculated by the method of the spherical excess as sum over the interior angles of the projection of the i-th patch on a unit sphere centered at $\vec{r} = \vec{c}_k$ [9]. Since eq. (16) is not solveable analytically in general [8] the outer integration can be approximated by an average over 9 triangular sub-patches of ΔS_k. A test evaluation showed that, compared with a (unacceptably time consuming) numerical double surface integration (16), the relative differences between (16) and (17)-(18) are neglectable in most cases. Even the simplest "naïve" method of approximating $\Omega_i(\vec{r}) \approx \cos\theta' \Delta S_i / R^2$ deviates from (17) by maximum 1% if $\Delta S_i / R^2 < 10^{-2}$ ("far" patch-patch distances).

Computation of time-dependent irradiation strengths: For the time-dependent RadM a time step Δt as average sound travelling time from one patch to its neighbor patch is defined by $\Delta t = \overline{L}_{pp}/c$ where $\overline{L}_{pp}$ is an average distance between the centroids of two adjacent patches. On the other hand, to allow a roughly sufficient temporal resolution, $\overline{L}_{pp}$ should be of the order of 1/10 of the room's mean free path length. The total iteration time T should be at least half the reverberation time T_{60} which can be estimated with Sabine's formula using the given ρ_i and ΔS_i.

The time iteration is executed for $N_t = \lceil T/\Delta t \rceil$ time steps; it describes the energy transfer and re-distribution process among the patches i.e. among the values of the matrix elements of B according to a time-discretized version of (15). There $B_k(t)$ results from the B_i and power P retarded in time. In an intuitive "future oriented" approach the irradiation strength B_{li} of patch i is distributed forward in time and space to patch k by adding its $(\rho_i g_{ik})$-fold to the respective element of matrix B. The sound travelling distance and time are R_x and R_x/c, thus the receiving row index in the matrix B is $m_x := l + \lceil R_x/(c\Delta t) \rceil$ and the sending row index is l. There

are four energy transfer processes to be executed iteratively acoording to equations (15) and (8), therefore $R_x = R_{sk},\ R_{ik},\ R_{ir},$ or R_{sr} (anologuously for m_x). Each is carried out for all time steps $l = 1,\ldots,N_t$.

"Source to wall": Distribute the source power to all patches (P-term in (15)): $B_{m_{s,k}k} \leftarrow B_{m_{s,k}k} + P_l \cos\theta_{s,k}/(4\pi R_{s,k})$.

"Wall to wall": For each patch i distribute its radiation strength to all patches k (B-term in (15)): $B_{m_{ik}k} \leftarrow B_{m_{ik}k} + g_{ik}\rho_i B_{li}$.

"Wall to receiver": For all patches i distribute their radiation strength to the receiver (B-term in (8)): $I_{m_{ir}} \leftarrow I_{m_{ir}} + g_{ir}\rho_i B_{li}$.

"Source to receiver": Distribute the source intensity to the receiver ((P-term in (8))): $I_{m_{sr}} \leftarrow I_{m_{sr}} + P_l/(4\pi R_{sr}^2)$.

4 NUMERICAL EXPERIMENTS

While the BEM needs impedances $\underline{Z}$ the RadM needs the corresponding reflection degrees $\rho = 1-\alpha$ (absorption degree α). The following relationship between them has been employed:

$$\alpha = \frac{8}{\zeta^2}\cos\mu\left[\zeta + \frac{\cos 2\mu}{\sin\mu}\arctan\left(\frac{\zeta\sin\mu}{1+\zeta\cos\mu}\right) - \cos\mu\ln\left(1+2\zeta\cos\mu+\zeta^2\right)\right],\quad \underline{\zeta} = \frac{\underline{Z}}{\rho_a c}, \tag{19}$$

where ζ and μ are absolute value and angle of the specific impedance $\underline{\zeta}$ [5].

4.1 Setup

The three investigated rooms were intended to be reverberation chambers according to ISO354 yet smaller to reduce the computational effort. Reverberation time T_{20} and the sound intensity level L were calculated once each with 2 absorption distributions and with both methods. In each of these 12 cases the receiver points were in 10 cm × 10 cm grids, one horizontal (z = 0.5 m), one vertical (x = 1.25 m). Source: point source at $\vec{r}_s = (2,2,1)^T$, power: $P = 1$ W total power of source impulse in BEM, RadM: $P_l = 1$ W for the first time step, else zero.

Rooms: 1. rectangular room with edge lengths of 4 m, 4.5 m, and 2.8 m (V = 50.4 m^3, S = 83.6 m^2); 2. a slanted room created from the rectangular room by tilting 3 surfaces by 4° inwards (V = 44.5 m^3, S = 77.3 m^2); 3. a room with pentagonal floor plane and without any pair of parallel walls (V = 41.0 m^3, S = 71.7 m^2). Additionally the rectangular room was transformed to a room with "rough" and hence scattering walls by shifting all patch vertices perpendicular to the surface by equally distributed random distances between 0 and $\overline{L}_{pp}$ (for BEM only as the surface is inherently scattering perfectly in the RadM).

Absorption distributions: 1. All specific wall impedances $\underline{\zeta}$ were set to $0.008 + 0.2889\,j$, all absorption coefficients ρ for RadM were set to the corresponding value 0.98 (19). 2. As absorber a 2.5m×3.5m rectangular area at the floor with ≥ 0.5 m distance from all vertical walls, where $\underline{\zeta} = 3.0880 + 1.3170\,j$ (BEM, mass-damper-like) and $\rho = 0.2$ (RadM).

Tesselation: BEM: ≈ 20,000 patches, mean distance $\overline{L}_{pp}$ = 9.5 cm, max. distance <15 cm; RadM: ≈ 5,000 patches, mean distance $\overline{L}_{pp}$ = 20 cm, max. distance <32 cm.

With the BEM $\underline{p}(\vec{r}_r, f)$ was calculated for the frequencies 170 Hz to 360 Hz in steps of 0.25 Hz (length 4 s FIR) and, after inverse Fourier transform, 250 Hz octave band filtered. Thus the number of patches was suitable for the BEM though the calculation times were still manageable (≈ 600 s per frequency in MATLAB, 4 core CPU at 2 GHz with 16 GB RAM). The resulting impulse response was Schroeder-backwards-integrated to determine the energy-time-decay curves. With the RadM the resulting $I(\vec{r}_r)$ from an impulse experiment were backward-integrated without any previous transform.

4.2 Results and conclusions

The attempted results are shown as an overview in table 1.

Table 1. Reverberation time T20 and sound level L (mean $\pm$ standard derivation) taken over all receiving points

room	L [dB]		T20 [s]		T60 [s]	
	BEM	RadM	BEM	RadM	Eyring	Sabine
rectangular without absorber	90.8 $\pm$ 1.1	92.1 $\pm$ 2.2	5.9 $\pm$ 0.3	4.6 $\pm$ 0.0	4.8	4.8
rectangularwith absorber	84.6 $\pm$ 2.0	86.0 $\pm$ 2.1	2.7 $\pm$ 0.5	1.0 $\pm$ 0.0	1.1	1.1
rough rectangular without absorber	91.1 $\pm$ 1.1	—-	8.3 $\pm$ 0.4	—-	4.2	4.3
slanted without absorber	91.7 $\pm$ 1.1	93.0 $\pm$ 2.0	6.0 $\pm$ 0.5	4.4 $\pm$ 0.0	4.6	4.6
slanted with absorber	84.3 $\pm$ 1.8	87.6 $\pm$ 2.0	2.2 $\pm$ 0.3	0.9 $\pm$ 0.0	1.0	1.0
pentagonal without absorber	91.6 $\pm$ 1.6	93.4 $\pm$ 2.3	5.7 $\pm$ 0.3	4.3 $\pm$ 0.0	4.5	4.6
pentagonal with absorber	83.8 $\pm$ 2.1	86.7 $\pm$ 2.2	1.8 $\pm$ 0.2	0.9 $\pm$ 0.0	0.9	1.0

Primarily, the results indicate that in the BEM – as in reality – local areas of high absorption lead to longer reverberation times than predicted in Sabine's formula which can be explained by the "survival" of long distance reflected "sound particles".

It is remarkable that, in BEM, the inhomogeneity of the sound field due to rooms modes can be recognized in reverberation times even though these are defined as a relative decay only (figures 2 and 3). This effect also occurs with the rooms with tilted walls.

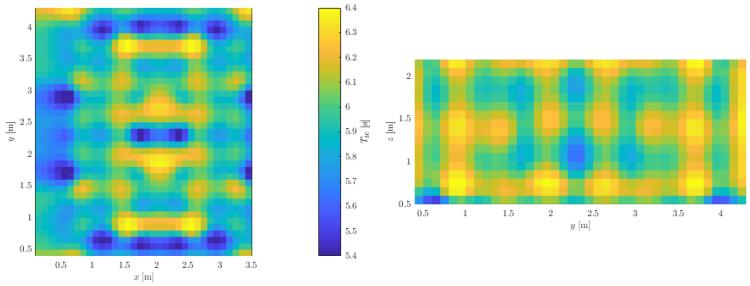

Figure 2. Reverberation time T_{20} of the rectangular room without absorber; a) horizontal, b) vertical grid of receiving points

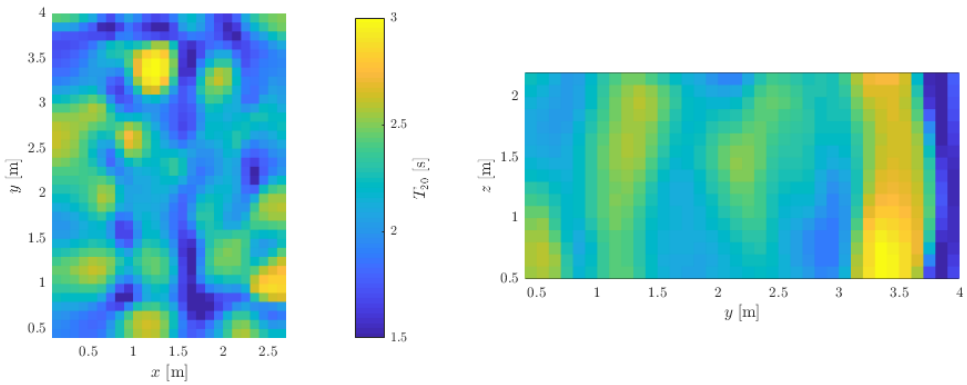

Figure 3. Reverberation time T_{20} of the slanted room with absorber; a) horizontal, b) vertical grid of receiving points

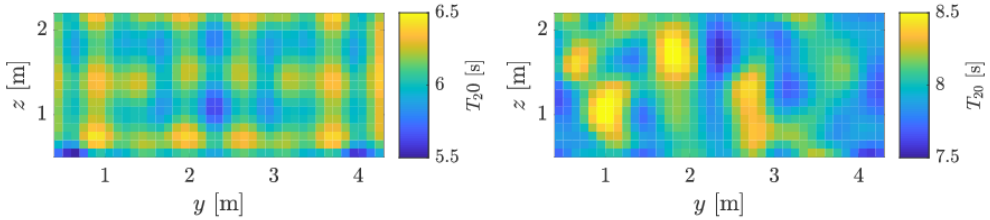

Figure 4. Reverberation time T_{20} at vertical plane of receivers in the rectangular room without absorber, a) even walls, b) rough walls

The influence of the room shape is small as compared to the effect of the absorber (table 1). Generally the influence of the absorption area is stronger in BEM than in RadM.

Surprisingly, there was no double slope effect in the sound decay curves as expected for non diffuse sound fields; the computed sound level decay curves were mostly straight lines (therefore not depicted).

The distributions and the values of the absorption coefficients were chosen to disturb the homogeneity and diffusity of the sound field violating the conditions under which Sabine's formula is valid. This should lead to higher T_{20} than according to Sabine. The results of the RadM instead indicate that perfectly scattering walls homogenize the sound field (standard deviations in table 1, column 4) so that RadM yields reverberation times as predicted by Sabine's and Eyring's formulas which strongly assume constant irradiation strengths. This may lead to an underestimation of T_{60} and thus an overestimation of the absorption coefficient as often occurs in measurements. As expected, the reverberation times computed by BEM are much longer than those from Eyring and RadM because of the rather geometrical reflections implicitely assumed in the BEM.

Astonishingly, the "crumpling" of the rough and scattering walls does not decrease but increase the reverbaration times resulting from the BEM (see the 8.3 s in table 1). In comparing BEM and RadM many effects and their reasons still have to be investigated.

REFERENCES

[1] Wu, T.-W.; Boundary Element Acoustics Fundamentals and Computer Codes, WIT Press, Boston, 2000.

[2] Marburg, S.; Schneider, S.; Vorländer, M.; Romanenko, G.: Boundary Elements for room acoustics; In: Proceedings. of Inter-Noise 2003, Jeju, Seogwipo (Korea), August 25 - 28, 2003

[3] Stephenson, U.M.; Comparison of the Mirror Image Source Method and the Sound Particle Simulation Method. Applied Acoustics 29 (1990), H.1, S. 35-72.

[4] Stephenson, U.M.: The differences and though the equivalence in the detection methods of particle, ray and beam tracing; Proceedings of ICA, Montreal (Canada), 2013

[5] Kuttruff, H.; Room Acoustics, lsevier Science Publishers Ltd., Barking (England), 3rd ed., 1991.

[6] Kuttruff, H. A Simple Iteration Scheme for the Computation of Decay Constants in Enclosures with Diffusely Reflecting Bondaries, J. Acoust.Soc. Am., Vol 98 (1), 1995, pp 288-293.

[7] Glassner, A. (ed.), An Introduction to Ray Tracing, Academic Press Ltd. London, San Diego, 1990.

[8] Miles, R.N. Sound Field in a Rectangular Enclosure with Diffusely Reflecting Boundaries; J. Sound. Vib. 92, 1984, pp 203-213

[9] Nosal, E.-M. Improved algorithms and methods for room sound-field prediction by acoustical radiosity in arbitrary polyhedral rooms, J. Acoust. Soc. Am., Vol 116 (2), 2004, pp 970-980.